Effects of Helium and Carbon-Dioxide Dilutions on Hydrogen Jet Ignition in a Shock Tube

Marcel Martins Alves, Odai Nassar
Tel Aviv University, School of Mechanical Engineering
Tel Aviv, Israel

Sergey Kudriakov, Etienne Studer
DES/ISAS-DM2S-STMF, CEA, Université Paris-Saclay
Gif-sur-Yvette, France

Liel Ishay
Nuclear Research Center Negev
Negev, Israel

Yoram Kozak
Tel Aviv University, School of Mechanical Engineering
Tel Aviv, Israel

1 Introduction

Research on hydrogen combustion is important for the mitigation of hydrogen accidental explosions [1]. Hydrogen is usually stored at high pressures and, in case there is an accidental leakage of a hydrogen jet from a high-pressure vessel into the atmosphere, there is formation of a shock wave and a contact surface [2]. The shock wave raises both pressure and temperature of the gas downstream of it. In addition, in the expansion process, the temperature of the hydrogen jet drops. Moreover, there is mixing between the hot air and the cold hydrogen at the contact surface, also referred to as diffusion layer [2, 3]. Because hydrogen has a low Lewis number, i.e., high diffusion coefficient, it diffuses into the hot air region downstream of the shock wave [3]. Therefore, ignition should occur if the temperature rise caused by the chemical reactions is higher than the temperature drop caused by the jet expansion [2].

Hydrogen jet ignition is investigated experimentally in shock tubes [4]. A shock tube consists of a driver section, a driven section, and a diaphragm. The diaphragm can be a metal piece and it separates the driver and driven sections [5]. The driver section and driven section are also referred to as high-pressure chamber and low-pressure chamber, respectively. In a shock-tube experiment, as the driver section is filled with gas, the diaphragm bulges towards the driven section [6]. Eventually, the diaphragm ruptures and a jet propagates through the diaphragm opening into the driven section as the diaphragm tears and folds backwards [5]. In this process, compression waves form in the driven section, and eventually overtake each other and coalesce to form a shock front [5, 6].

Correspondence to: mmalves@tauex.tau.ac.il

The diaphragm rupture may also occur partially [7]. In these cases, the diameter of the diaphragm rupture, also referred to as diaphragm opening, is lower than the shock-tube diameter for a round cross-sectional area shock tube. Therefore, there is a diameter ratio between the diaphragm opening and the shock-tube cross section, d/D, and an area ratio between the diaphragm opening and the shock-tube cross section, a/A [7].

A theoretical model was developed in [8] to calculate the gas properties throughout the shock tube in cases of a partially opened diaphragm. The model from [8] uses a discharge coefficient for flows past an orifice plate in order to account for stagnation pressure losses in the flow region near the diaphragm. Equations from the 1D simple shock-tube theory [9, 10] are also used in the model from [8]. Moreover, the model from [8] calculates the shock-wave Mach number at the distance of $3D$ (three tube diameters) from the diaphragm and the gas properties downstream of the shock wave at this location. This location was chosen based on the fact that the shock wave becomes nearly planar at the distance of $3D$ [7].

Initially, a discharge coefficient for incompressible flows past a concentric orifice plate with a vena contracta tap, C_{di}, is calculated in the model from [8] in Equation 1 [11], where $b = 0.00025 + 0.002325(\sqrt{a/A} + 1.75(a/A)^2 + 10(a/A)^6 + 2(D_{\mathrm{H}})(a/A)^8)$; $D_1 = (D_{\mathrm{H}}/0.0254)^2(a/A) + 0.01\,(D_{\mathrm{H}}/0.0254)$; and $\lambda = 1000/\sqrt{\mathrm{Re}_H}$. In addition, D_{H} and Re_H are the hydraulic diameter of the driver section and the Reynolds number of the gas in the driver section, respectively. Equation 1 is applicable for $D_{\mathrm{H}} \geq 0.0429$ m, $\mathrm{Re}_H > 10^4\sqrt{a/A}$, and $0.04 < a/A < 0.5625$, which imposes an applicability range in the model from [8].

$$C_{\mathrm{di}} = \left[b\lambda + 0.5922 + 0.4252\left(\frac{0.0006}{D_1} + \left(\frac{a}{A}\right)^2 + 1.25\left(\frac{a}{A}\right)^8\right)\right]\sqrt{1 - \left(\frac{a}{A}\right)^2} \tag{1}$$

Moreover, the discharge coefficient for incompressible flows, calculated in Equation 1, is converted into a discharge coefficient for compressible flows in the model from [8] by using Equation 2 [12, 13], where $f = 1/C_{\mathrm{di}} - 1/(2C_{\mathrm{di}}^2)$; $r = P_{\mathrm{b}}/P_0 = P_1/P_4$; $r_{\mathrm{c}} = (2/(\gamma_4 + 1))^{\gamma_4/(\gamma_4 - 1)}$; $r_1 = (r_{\mathrm{c}} - r)(r_{\mathrm{c}})^{1/\gamma_4}$; $K_{\mathrm{N}}^2 = \gamma_4(2/(\gamma_4 + 1))^{(\gamma_4+1)/(\gamma_4-1)}$; P_1 is the initial pressure of the driven gas; P_4 is the initial pressure of the driver gas; and γ_4 is the ratio of specific heats of the driver gas.

$$C_{\mathrm{d}} = \frac{1}{2f(r_{\mathrm{c}})^{1/\gamma_4}}\left\{\left[1 + \frac{r_1}{K_{\mathrm{N}}^2}\right] - \sqrt{\left[1 + \frac{r_1}{K_{\mathrm{N}}^2}\right]^2 - \left[\frac{4(r_{\mathrm{c}})^{2/\gamma_4}(1 - r)f}{K_{\mathrm{N}}^2}\right]}\right\} \tag{2}$$

The gas regions in the model from [8] are shown in Figure 1, where state 4 is the initial driver gas, state 3 is the expanded driver gas in the driver section, region 3a is the expanding driver gas in the driver section, j is the vena contracta, region 2a is the expanding driver gas in the driven section, region 2b is the expanded driver gas in the driven section, state 2 is the gas downstream of the shock wave, and state 1 is the pre-shock gas. The model from [8] considers an isentropic expansion between state 3 and j. Moreover, the model is only valid if the flow becomes sonic in j; and the model assumes that the mass flow rate is constant between state 3, j, and region 2b.

The model from [8] uses arbitrary values for a/A; therefore, diaphragm physical properties are not accounted for in the calculation of a/A in [8]. The present work uses a new theoretical method to account for the effects of diaphragm properties on a/A. Therefore, realistic values of a/A are calculated in the present work. Then, we investigate the effects of diaphragm thickness, driver-gas dilution, and driven-gas dilution on the gas region downstream of the shock wave, state 2. It is important to point out that chemical reactions, which may lead to ignition, occur in state 2 in shock-tube experiments. Therefore, it is important to investigate the gas properties in this region.

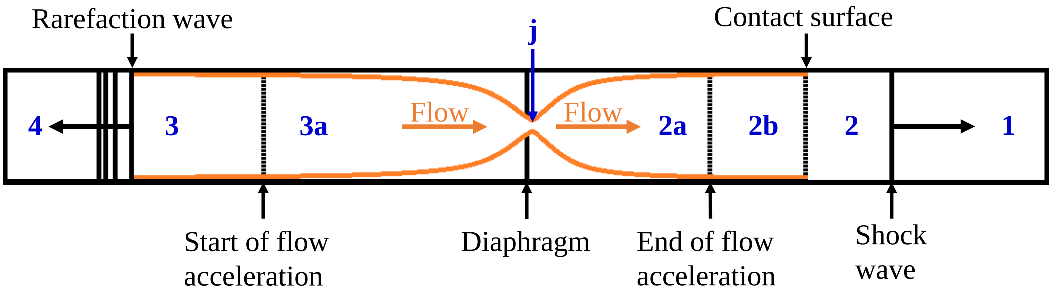

Figure 1: Schematic of the model setup from [8].

2 Methodology

A round cross-sectional-area shock tube with a diameter, D, equal to 0.10 m is considered in the present work. The diaphragm material is nickel. The initial pressure of the driven gas (P_1) is equal to 101325 Pa. The initial pressure ratio across the diaphragm (P_4/P_1) is equal to 640. The initial temperature of both driver (T_4) and driven (T_1) gases is equal to 298 K. Moreover, the diaphragm material, P_1, P_4/P_1, T_4, and T_1 are the same in all cases investigated in the present work.

In order to investigate the effects of driver-gas dilution on the temperature in state 2 (T_2), see Figure 1, different gas mixtures of hydrogen (H_2), helium (He), and carbon dioxide (CO_2) are considered as respective driver gases, as shown in Table 1, where X_{H_2}, X_{He}, and X_{CO_2} are the mole fractions of H_2, He, and CO_2, respectively, R_4 is the driver-gas constant in J/(kg·K), and c_4 is the speed of sound of the driver gas in m/s.

Table 1: Driver-gas properties, driven-gas properties, and 1D-theory solution.

Driver gas	X_{H_2}	X_{He}	X_{CO_2}	γ_4	R_4	c_4	Driven gas	X_{Air}	X_{He}	X_{CO_2}	γ_1	R_1	c_1	$T_2\|_{1D}$	$M_s\|_{1D}$
H_2	1.0	0.0	0.0	1.40	4124	1312	Air	1.0	0.0	0.0	1.40	287	346	3018	6.87
H_2/He	0.95	0.05	0.0	1.41	3930	1285	Air	1.0	0.0	0.0	1.40	287	346	2922	6.75
H_2/He	0.90	0.10	0.0	1.42	3754	1260	Air	1.0	0.0	0.0	1.40	287	346	2833	6.64
H_2/He	0.85	0.15	0.0	1.43	3593	1237	Air	1.0	0.0	0.0	1.40	287	346	2749	6.53
H_2/He	0.80	0.20	0.0	1.44	3445	1216	Air	1.0	0.0	0.0	1.40	287	346	2670	6.42
H_2/CO_2	0.95	0.0	0.05	1.40	2020	918	Air	1.0	0.0	0.0	1.40	287	346	2067	5.55
H_2/CO_2	0.90	0.0	0.10	1.39	1338	744	Air	1.0	0.0	0.0	1.40	287	346	1677	4.91
H_2/CO_2	0.85	0.0	0.15	1.38	1000	641	Air	1.0	0.0	0.0	1.40	287	346	1454	4.50
H_2/CO_2	0.80	0.0	0.20	1.37	798	571	Air	1.0	0.0	0.0	1.40	287	346	1307	4.21
H_2	1.0	0.0	0.0	1.40	4124	1312	Air/He	0.95	0.05	0.0	1.41	300	355	3010	6.78
H_2	1.0	0.0	0.0	1.40	4124	1312	Air/He	0.80	0.20	0.0	1.43	347	385	2900	6.50
H_2	1.0	0.0	0.0	1.40	4124	1312	Air/He	0.60	0.40	0.0	1.48	438	440	2803	6.06
H_2	1.0	0.0	0.0	1.40	4124	1312	Air/CO_2	0.95	0.0	0.05	1.39	280	341	2993	6.92
H_2	1.0	0.0	0.0	1.40	4124	1312	Air/CO_2	0.80	0.0	0.20	1.37	260	326	2977	7.08
H_2	1.0	0.0	0.0	1.40	4124	1312	Air/CO_2	0.60	0.0	0.40	1.35	238	309	2974	7.26

The effects of driven-gas dilution on the temperature in state 2, see Figure 1, are investigated by considering different gas mixtures of air, He, and CO_2 as respective driven gases, as shown in Table 1, where X_{Air} is the mole fraction of air, γ_1 is the ratio of specific heats of the driven gas, R_1 is the driven-gas constant in J/(kg·K), and c_1 is the speed of sound of the driven gas in m/s. Moreover, the 1D-theory solution [10] for each case is shown in Table 1, where $T_2|_{1D}$ is the gas temperature in state 2 and $M_s|_{1D}$ is the shock-wave Mach number.

The extent of the diaphragm opening, i.e., the opening diameter (d), is calculated in Equation 3 [14], where t_d is the diaphragm thickness, f_ult is the ultimate stress of the diaphragm material, and ΔP is the pressure difference between the driver gas and the driven gas that causes the diaphragm rupture, calculated as $\Delta P = P_4 - P_1$. The ultimate stress of nickel is 480 MPa [15].

$$d = \frac{4 t_\mathrm{d} f_\mathrm{ult}}{\Delta P} \tag{3}$$

Based on the values of d calculated in Equation 3 and D; a/A values are calculated as a function of t_d and then implemented in the model from [8]. In shock-tube experiments, a rigid plate with an open area is placed on the diaphragm in order to control a/A [7]. In this manner, the diaphragm opening area corresponds to the open area of the rigid plate; and there is a measurement of P_4/P_1 required to rupture the diaphragm [7].

3 Results

The results for d/D for the driver gases and driven gases from Table 1 are shown in Figure 2. Because Equation 3 is not a function of the gas composition, the driver-gas and driven-gas dilutions do not affect the opening diameter, d. As a result, d/D is the same at a specific t_d for all cases from Table 1. Moreover, Figure 2 shows a linear increase in d/D as t_d increases, which is explained by the linear relationship between t_d and d in Equation 3.

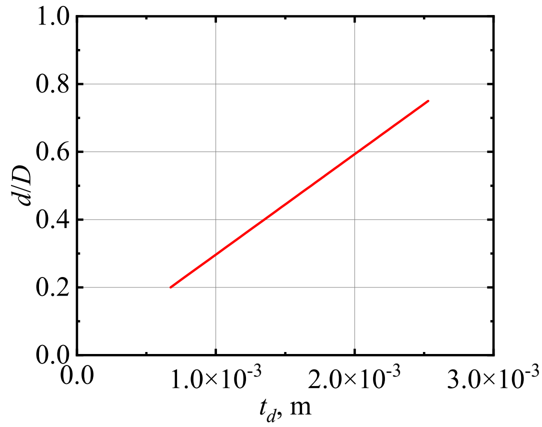

Figure 2: Diameter ratio as a function of t_d for P_4/P_1 = 640.

Dilution of H_2 with He or CO_2 decreases the gas speed of sound when compared to pure H_2 (see Table 1). Therefore, respective driver-gas dilutions of H_2 with He and CO_2 produce weaker shocks than the case of pure H_2 as a driver gas, which is observed in $T_2|_\mathrm{1D}$ and $M_s|_\mathrm{1D}$ in Table 1 and in Figure 3 (Left) for He and Figure 3 (Right) for CO_2. For example, for $t_\mathrm{d} = 2.5 \times 10^{-3}$ m, T_2 is decreased by 12% and 58% for X_He=0.20 and $X_{\mathrm{CO_2}}$=0.20, respectively, when compared to the case of pure H_2 as a driver gas (X_He=0.0 and $X_{\mathrm{CO_2}}$=0.0). However, the temperature drop caused by the driver-gas dilution gradually decreases with a reduction in t_d (i.e., lower a/A and therefore weaker shock). For example, for $t_\mathrm{d} = 6.7 \times 10^{-4}$ m, X_He=0.20 and $X_{\mathrm{CO_2}}$=0.20 lead to a temperature decrease by 5% and 37%, respectively, when compared to pure H_2 as a driver gas.

The respective driven-gas dilutions of air with He and CO_2 lead to changes in the speed of sound of the driven gas when compared to the case of pure air as a driven gas (see Table 1). For X_He=0.40, the speed of sound is higher than for the case of pure air as a driven gas by 27%. As a result, there is a temperature decrease by 7% at $t_\mathrm{d} = 2.5 \times 10^{-3}$ m for X_He=0.40 when compared to the case of pure air (X_He=0.0) as a driven gas, as shown in Figure 4 (Left). In regard to the driven-gas dilutions with CO_2, it is shown in Figure 4 (Right) that T_2 is reduced by up to 4% for X_{CO_2}=0.40 when compared to the case of pure air (X_{CO_2}=0.0) as a driven gas, which is explained by the fact that the speed of sound for this gas mixture is only lower than the speed of sound for pure air by 11%.

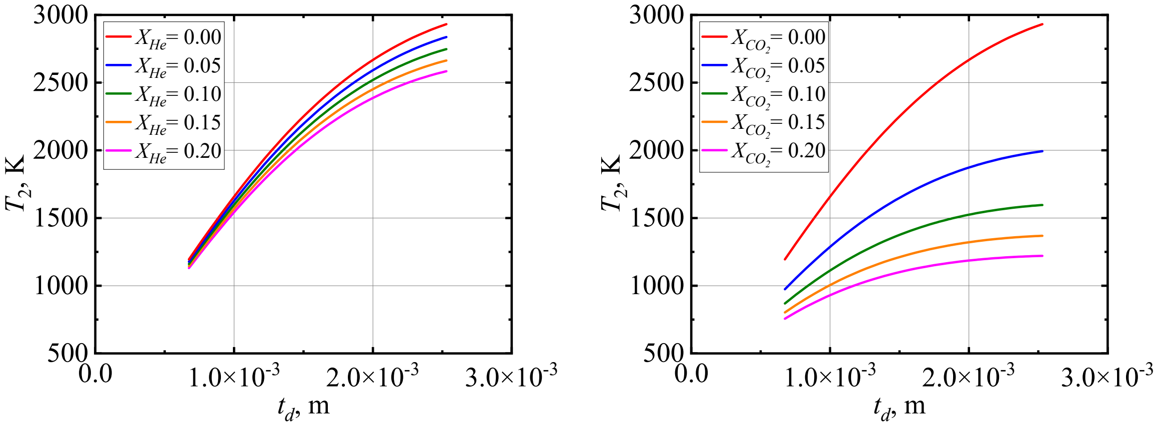

Figure 3: Temperature profiles in state 2 as a function of t_d for different driver gases. Left: H_2/He dilutions. Right: H_2/CO_2 dilutions.

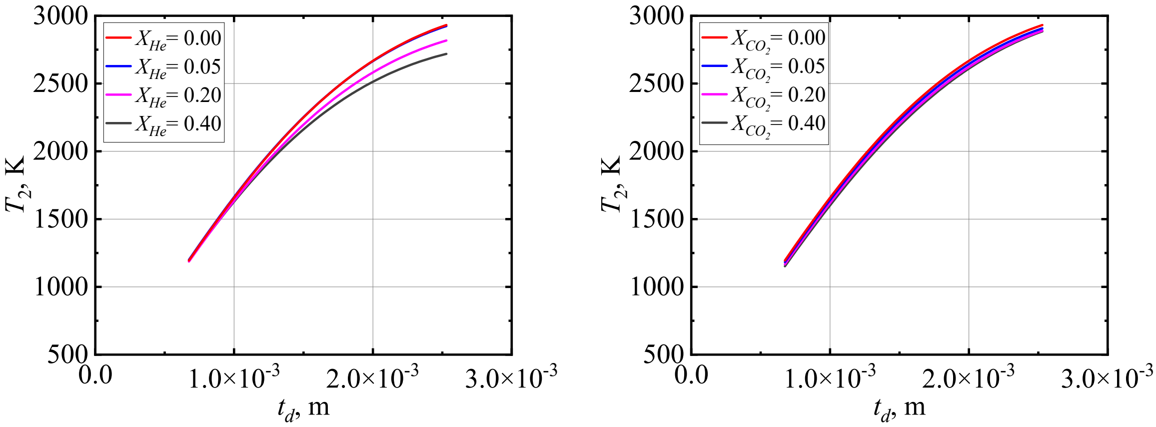

Figure 4: Temperature profiles in state 2 as a function of t_d for different driven gases. Left: Air/He dilutions. Right: Air/CO_2 dilutions.

4 Conclusions

A new method was used in the present work in order to investigate theoretically the effects of the diaphragm properties, such as material and thickness, on the gas temperature in the region downstream of the shock wave (T_2) in a round cross-section shock tube with a diameter equal to 0.10 m and a partially opened nickel diaphragm at conditions of hydrogen jet ignition experiments (i.e., $P_4/P_1 = 640$). Furthermore, dilution effects of both driver gas and driven gas with He and CO_2 were investigated. It was found that a large dilution of air with He (i.e., X_{He}=0.40) as a driven gas can only reduce T_2 by 7% for a diaphragm with $t_d = 2.5 \times 10^{-3}$ m when compared to the case of pure air as a driven gas. On the other hand, driver-gas dilutions with He and CO_2 can lead to significant reductions in T_2 when compared to the case of pure H_2 as a driver gas. For example, for $t_d = 2.5 \times 10^{-3}$ m, X_{He}=0.20 and X_{CO_2}=0.20 lead to a reduction in T_2 by 12% and 58%, respectively, when compared to the case of pure

H_2 as a driver gas. Future work will be carried out in order to compare the new method used in the present work with experimental results from the literature.

5 Acknowledgments

The authors would like to acknowledge the NRCN-CEA International Collaboration Research Fund and the Pazy Foundation for funding this research.

References

[1] Mogi T, Wada Y, Ogata Y, Hayashi AK. (2009). Self-ignition and flame propagation of high-pressure hydrogen jet during sudden discharge from a pipe. Int. J. Hydrog. Energy. 34: 5810.

[2] Maxwell BM, Radulescu M.I. (2011). Ignition limits of rapidly expanding diffusion layers: Application to unsteady hydrogen jets. Combust. Flame. 158: 1946.

[3] Bourgin E, Alves MM, Yang C, Fachini FF, Bauwens L. (2017). Effects of Lewis numbers and kinetics on spontaneous ignition of hydrogen jets. Proc. Combust. Inst. 36: 2833.

[4] Burke MP, Chaos M, Ju Y, Dryer FL, Klippenstein SJ. (2012). Comprehensive H2/O2 kinetic model for high-pressure combustion. Int. J. Chem. Kinet. 44: 444.

[5] White DR. (1958). Influence of diaphragm opening time on shock-tube flows. J. Fluid Mech. 4: 585.

[6] Henshall BD. (1955). On some aspects of the use of shock tubes in aerodynamic research. Aeronautical Research Council Reports and Memoranda 3044.

[7] Gaetani P, Guardone A, Persico G. (2008). Shock tube flows past partially opened diaphragms. J. Fluid Mech. 602: 267.

[8] Alves MM, Johansen CT. (2021). Modeling shock-wave strength near a partially opened diaphragm in a shock tube. Shock Waves. 31: 499.

[9] Liepmann HW, Puckett AE. (1947). Introduction to aerodynamics of a compressible fluid. John Wiley and Sons.

[10] John JEA, Keith TG. (2006). Gas dynamics. Pearson Prentice Hall.

[11] Emerson Process Management. (2005). Flowel 4 development and marketing. User Manual Emerson Project 3007536.

[12] Jobson DA. (1955). On the flow of a compressible fluid through orifices. Proc. Inst. Mech. Eng. 169: 767.

[13] Morris SD. (1990). Discharge coefficients for choked gas-liquid flow through nozzles and orifices and applications to safety devices. J. Loss Prev. Process. Ind. 3: 303.

[14] Glass II, Hall JG. (1959). Handbook of supersonic aerodynamics, section 18, shock tubes. Navord Report 1488 6.

[15] Callister WD. (2007). Materials science and engineering: An introduction. John Wiley and Sons.